ELSEVIER

NDT&E International 34 (2001) 219–226

NDT&E international

www.elsevier.com/locate/ndteint

Scan of surface-opening cracks in reinforced concrete using transient elastic waves

P.-L. Liu*, K.-H. Lee, T.-T. Wu, M.-K. Kuo

Institute of Applied Mechanics, National Taiwan University, Taipei, Taiwan, ROC

Abstract

This study develops a method to scan the surface cracks of reinforced concrete using transient elastic wave tests. In the tests, an impact is applied at constant intervals along one side of the crack opening, and the surface response of the concrete due to each impact is measured and recorded. Then the procedure is repeated with the source applied on the opposite side. The method of ellipse intersection is adopted to process the surface response of the concrete structure. An image is then constructed that shows the three-dimensional image of the crack. The image can be used to determine the location of the reinforcing steel bars, the thickness of the covering, and to judge whether the crack penetrates through the rebars. Numerical examples and a model test are presented to verify the effectiveness of this method. © 2001 Elsevier Science Ltd. All rights reserved.

Keywords: Surface-opening cracks; Reinforced concrete; Transient elastic waves; Imaging

1. Introduction

Reinforced concrete is the most commonly used construction material now-a-days. Since the tensile strength of concrete is only about 10% of its compressive strength, cracks often develop in concrete. If the cracks penetrate through the rebars, the rebars may deteriorate due to corrosion. As such, the strength of the structure is decreased and failure of the structure may follow. Therefore, the detection of cracks in reinforced concrete is indispensable in the safety assessment of reinforced concrete structures.

Recently, stress waves have been widely used to detect surface opening cracks in concrete. Sakata and Ohtsu [1] applied ultrasonic spectroscopy to evaluate vertical cracks. Chang and Wang [2] used ultrasonic waves to scan surface opening cracks. In addition to ultrasonic waves, many researchers have adopted transient elastic wave tests in the detection of cracks in concrete. Wu et al. [3] developed an inverse method to detect the depth of vertical cracks based on phase information. Lin and Su [4] and Lin et al. [5] applied the impact echo method to measure the depth of cracks in reinforced concrete. Liu et al. [6] proposed a migration imaging method that can depict the location of a surface-opening crack on a test section. Kuo et al. [7] applied optimization techniques to locate the crack tip.

This study is an extension of the two-dimensional imaging method by Liu et al. [6]. It aims at developing a method to scan the surface cracks of reinforced concrete using transient elastic wave tests. Different from Chang and Wang [2], the proposed method can construct a three-dimensional image of the crack. Furthermore, based on the image, one can determine the location of the reinforcing steel bars, the thickness of the covering, and judge whether the crack penetrates through the rebars.

2. Imaging of cracks in plain concrete

Consider a concrete block with a surface-opening crack of constant length. Select a test section that is perpendicular to the crack opening. When a source is applied on the surface at one side of the crack opening, elastic waves are generated and propagated in the concrete block. Waves reaching the crack will be reflected and the waves reaching the crack tip will be diffracted and arrive at the other side of the crack. A receiver mounted on the opposite side of the crack opening can receive diffracted signals from the crack tip. Suppose the travel time of the diffracted signal is t and the wave velocity is v. Then the travel distance of the signal is vt. If the diffraction path is unknown, any point in the block with the same travel distance is a possible diffraction point. Therefore, the diffraction point should fall on an ellipse with the source and receiver as its foci as shown in Fig. 1. If two ellipses are drawn using different diffracted signals, the diffraction point must be located at the

* Corresponding author. Fax: +886-2-2363-9290.
E-mail address: peiling@spring.iam.ntu.edu.tw (P.-L. Liu).

PII: S0963-8695(00)00061-X

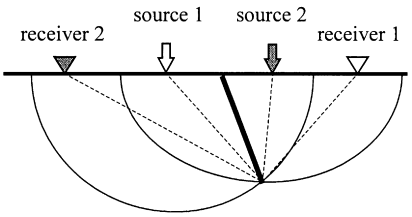

Fig. 1. Intersection of ellipses.

intersection of the two ellipses. Connecting the crack opening and the intersection, one obtains an image of the crack on the test section as shown in Fig. 1.

Move the source and receiver along the crack opening to a new test section, and perform the test again as shown in Fig. 2. One can obtain a crack image of the new section. Repeating the procedure several times, one obtains a sequence of crack images. A 3D image of the crack can be constructed simply by connecting all the 2D crack images in a 3D draw.

Notice that when the length of the crack varies, the image method needs to be modified since the diffraction point does not necessarily fall on the test section. The modification can be accomplished by solving an optimization problem. The details can be found in the work by Lee [8].

3. Influence of reinforcing bars

The method proposed in the preceding section can construct the image of a surface crack in pure concrete successfully. However, when there is reinforcement in the concrete, the signals are influenced by the rebars. Longitudinal waves propagate much faster in steel bars than in concrete. Therefore, the first arrival does not necessarily come from the crack tip.

Suppose the crack has a dip angle ϕ and a constant length l. The rebar has a covering thickness H and radius b and it is perpendicular to the crack opening. Select a coordinate system such that the x–y plane coincides with the top surface of the concrete, and the x and y axes are, respectively, parallel to the rebar and the crack opening, as shown in Fig. 2. Suppose the test section is deviated from the rebar at a distance d and the coordinates of the source and receiver are $(s,d,0)$ and $(r,d,0)$, respectively. Then the travel time of the diffracted signal from the crack tip is

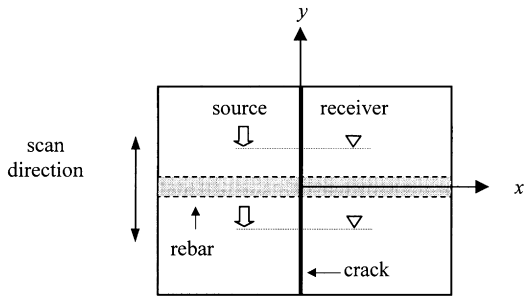

Fig. 2. Scan of crack.

$$t_{\text{crack}} = \frac{\sqrt{(s - l\sin\phi)^2 + (l\cos\phi)^2} + \sqrt{(r - l\sin\phi)^2 + (l\cos\phi)^2}}{C_{\text{p}}} \tag{1}$$

where C_{p} is the longitudinal wave speed of the concrete.

There are four other possible propagating paths for the first arrival, as shown in Fig. 3. In this figure, the source, receiver, and the intersection of the crack and the rebar are denoted as S, R, and I, respectively. In path (a), the signal emitting from S goes to I directly, and reflects back to R. In path (b), the signal goes to I first, then propagates along the rebar, and refracts back to R. In path (c), the signal refracts as it reaches the rebar, propagates along the rebar, then propagates from I back to R. In path (d), the signal refracts as it reaches the rebar, propagates along the rebar, and refracts back to R. The travel time of the signals from these paths are

$$t_{\text{a}} = \frac{\sqrt{(s - H\tan\phi)^2 + h^2} + \sqrt{(r - H\tan\phi)^2 + h^2}}{C_{\text{p}}} \tag{2}$$

$$t_{\text{b}} = \frac{\sqrt{(s - H\tan\phi)^2 + h^2} + \sqrt{\delta^2 + h^2}}{C_{\text{p}}} + \frac{|r - H\tan\phi| - \delta}{C_{\text{r}}} \tag{3}$$

$$t_{\text{c}} = \frac{\sqrt{(r - H\tan\phi)^2 + h^2} + \sqrt{\delta^2 + h^2}}{C_{\text{p}}} + \frac{|s - H\tan\phi| - \delta}{C_{\text{r}}} \tag{4}$$

$$t_{\text{d}} = \frac{2\sqrt{\delta^2 + h^2}}{C_{\text{p}}} + \frac{|r - s| - 2\delta}{C_{\text{r}}} \tag{5}$$

In these equations, C_{r} is the wave speed of the rebar,

$$h = \sqrt{d^2 + (H + b)^2} - b \tag{6}$$

is the shortest distance from the source (or receiver) to the rebar, and δ is the horizontal distance between the source (or receiver) and the refraction point at the rebar. δ can be expressed as

$$\delta = \frac{C_{\text{p}}h}{\sqrt{C_{\text{r}}^2 - C_{\text{p}}^2}} \tag{7}$$

One can show that the travel time of the refracted signal is always shorter than that of the direct wave through the concrete. However, refraction occurs only when the horizontal distance between the source (or receiver) and the intersection point of crack and rebar is greater than δ. Therefore, which path is the fastest depends on the geometry

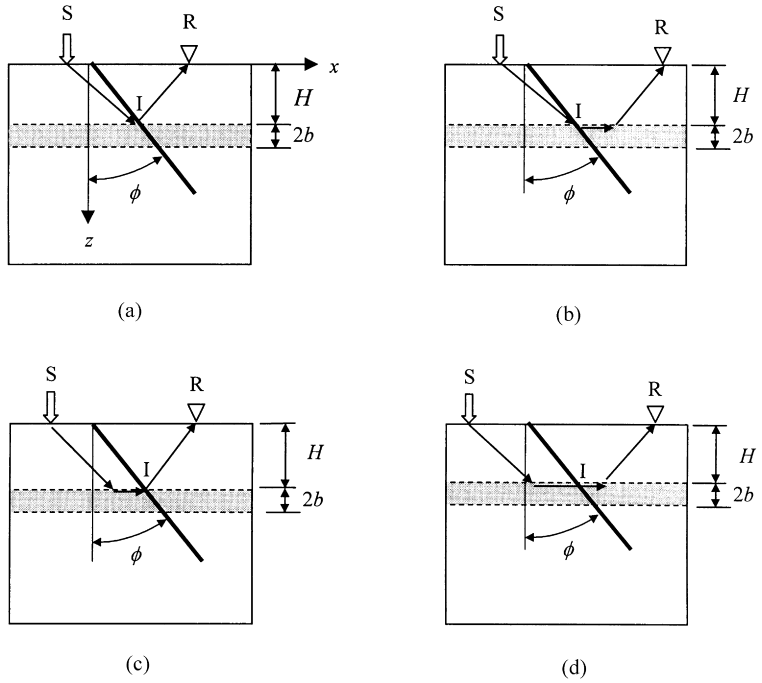

Fig. 3. Possible paths of the first arrival from the rebar: (a) $|s - H\tan\phi| < \delta$, $|r - H\tan\phi| < \delta$; (b) $|s - H\tan\phi| < \delta$, $|r - H\tan\phi| > \delta$; (c) $|s - H\tan\phi| > \delta$, $|r - H\tan\phi| < \delta$; (d) $|s - H\tan\phi| > \delta$, $|r - H\tan\phi| > \delta$.

of the test layout. For example, if $|H\tan\phi - s| < \delta$ and $|H\tan\phi - r| < \delta$, no refraction occurs. In that case, only path (a) is possible. If $|H\tan\phi - s| > \delta$ while $|H\tan\phi - r| < \delta$, then only one refraction may occur. Apparently, the signal cannot take path (b) or (d), and path (c) becomes the fastest.

If the first arrival comes from the rebar, it contains no information about the crack tip. In that case, the intersection of the ellipses no longer indicates the location of the crack tip. The sufficient conditions for the first arrival to come from the crack tip are

$$t_{\text{crack}} \le t_i, \qquad i = \text{a},\ldots,\text{d} \tag{8}$$

These are not necessary conditions because some of the paths may not be realizable. From these equations, one can derive the following expressions for the detectable length of the crack:

$$\bar{l}_i \frac{l_i}{H} = \frac{(\bar{r}+\bar{s})[(\bar{r}-\bar{s})^2 - \bar{t}_i^2]\sin\phi + \bar{t}_i\sqrt{[(\bar{r}-\bar{s})^2 - \bar{t}_i^2][\bar{r}^2 + (2 - 4\sin^2\phi)\bar{r}\bar{s} + \bar{s}^2 - \bar{t}_i^2]}}{2[(\bar{r}-\bar{s})^2\sin^2\phi - \bar{t}_i^2]} \tag{9}$$

where $\bar{r} = r/H$, $\bar{s} = s/H$, $\bar{t}_i = t_i C_p/H$, and $i = \text{a},\ldots\text{d}$. If $l < l_i$, then $t_{\text{crack}} \le t_i$ and the diffracted signal will arrive at the receiver earlier than the signal from path i.

In real applications, the actual length and dip angle of the crack are unknown. Hence, one cannot use Eq. (9) to check if the detected length is correct or not. However, one can still gain some insight by drawing l_i as a function of the distance d between the test section and the rebar.

Suppose $C_p = 4160$ m/s, $C_r = 5920$ m/s, $\bar{s} = 0.5$, $\bar{r} = -2$, $b/H = 0.25$, and $\phi = 0°$. The influence of d on the detectable length is shown in Fig. 4. If the normalized actual crack length l/H falls in the zone under all the curves, then Eq. (8) holds and the detected length is correct. If l/H falls in the zone above all these curves, the first arrival definitely comes from the rebar, and the detected length is thus too short. If l/H falls somewhere between the curves, the detected length may or may not be correct depending on the geometry of the test layout.

When the source and receiver are placed on top of the rebar, the crack length can be detected correctly only when $l/H < 1$, that is, only when the crack length is shorter than the covering thickness. This is obvious because when $l/H > 1$, the distance of path (a) is always shorter than that of the diffraction path. The detectable length increases as the test section departs from the rebar. This is expected because t_i grows with d while t_{crack} remains fixed. Therefore, the influence of the rebar is maximal when the source and receiver are placed on top of the rebar. The influence decreases as the test section is moved away from the rebar.

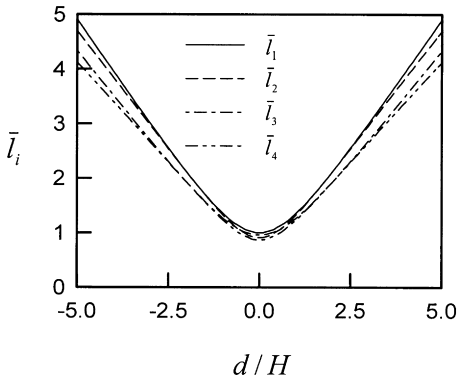

Fig. 4. Influence of test-section deviation on detectable length.

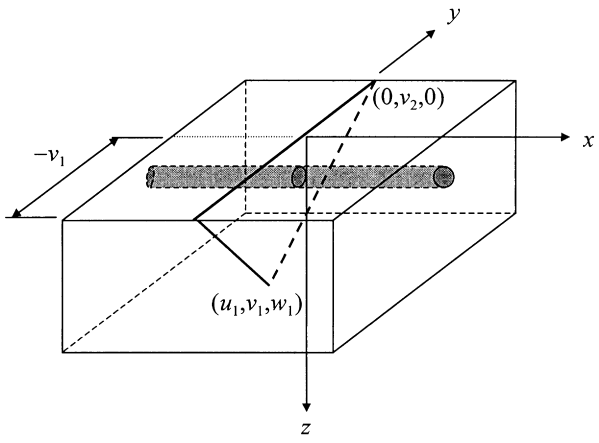

Fig. 5. Reinforced concrete block with a surface-opening crack.

Accordingly, the scan image of the crack may be distorted near the rebar and the distortion diminishes as the test section leaves the rebar. For example, if $l = 2H$, the crack length cannot be detected correctly if the test section is within $2.4H$ from the rebar (see Fig. 4). Hence, the scan image will be distorted in the range $|d| < 2.4H$. Although the image may be distorted, it still provides useful information. In the following, a few examples will be used to demonstrate the results of the scan.

4. Numerical examples

Consider a reinforced concrete block. The diameter of the rebar is 2 cm. The longitudinal wave velocities of the concrete and rebar are 4160 and 5920 m/s, respectively. The coordinate system is as shown in Fig. 5. Two test layouts were adopted for each test section. Unless specified otherwise, the source and the receiver were respectively located at $x = -2$ and 8 cm in the first test and at $x = 2$ and -8 cm in the second test. All test sections were perpendicular to the crack opening. In the scan, the test section was moved along the y-direction, and the distance between successive test sections was 1 cm.

4.1. Vertical crack with constant depth

Suppose a vertical crack exists in the reinforced concrete block. Assume that the crack is perpendicular to the rebar, and the depth of the crack tip is 8 cm. Fig. 6 shows the results of the scan for four different reinforcement conditions: (a) no rebar; (b) covering thickness of the rebar $H =$ 4 cm; (c) $H = 6$ cm and (d) $H = 8$ cm.

When there is no rebar, a correct image of the crack is constructed, as expected. On the other hand, the crack image is distorted when the rebar is present. The crack image remains plane. However, the crack edge is no longer a straight line. It becomes concave above the rebar and recovers straight when the test section is far away from the rebar as shown in Fig. 6(b) and (c). This phenomenon is due to the presence of the rebar as discussed in the previous section.

It should be noted that although the crack image seems to be correct as $H = 8$ cm, distortion still exists on top of the rebar. Since the crack does not penetrate through the rebar, one may expect the crack length to be detected accurately. However, $\delta = 7.9$ cm in this case. Comparing with s and r, one knows that the first arrival takes either path (b) or (c) when $d = 0$. Hence the detected length is $C_p t_2$ (or $C_p t_3$) = 7.9995 cm, not 8 cm. As the test section is 1 cm away from the rebar, the diffracted signal becomes the first to arrive. The detected length regains 8 cm.

Comparing Fig. 6(b)–(d), it is found that distortion of the image is reduced as the covering thickness increases. When $H = 4$ cm, the image is distorted when the test section is within 8 cm from the rebar. When $H = 6$ cm, the distortion range is reduced to 6 cm. When $H = 8$ cm, almost no distortion is observed. This trend is expected because the deeper the rebar is, the less likely the first arrival comes from the rebar.

Further inspection of Fig. 6(b) and (c) shows that consistent with Fig. 4, the crack length is shortest at the rebar location. Furthermore, the crack length at the rebar location is approximately equal to the covering thickness for both cases. In fact, if the first arrival takes path (a) in Fig. 3, the crack length is exactly the same as the covering thickness. However, the first arrival takes path (c). Hence, the travel time is a little shorter, so is the crack length.

The scan images in Fig. 6 were constructed using symmetric test layouts. Now consider the case where unsymmetrical test layouts are adopted. In the first test, the locations of the source and the receiver remain at $x = -2$ and 8 cm, respectively. In the second test, the source and the receiver are moved to $x = 6$ and -4 cm, respectively. Fig. 7 shows the results of the scan for two reinforcement conditions: (a) no rebar, and (b) $H = 4$ cm.

When no rebar is present, the image still shows a vertical crack plane with constant depth. When the rebar is present, the crack edge becomes concave. Furthermore, the crack image warps and is no longer a vertical plane. This is different from the case of symmetric test layouts.

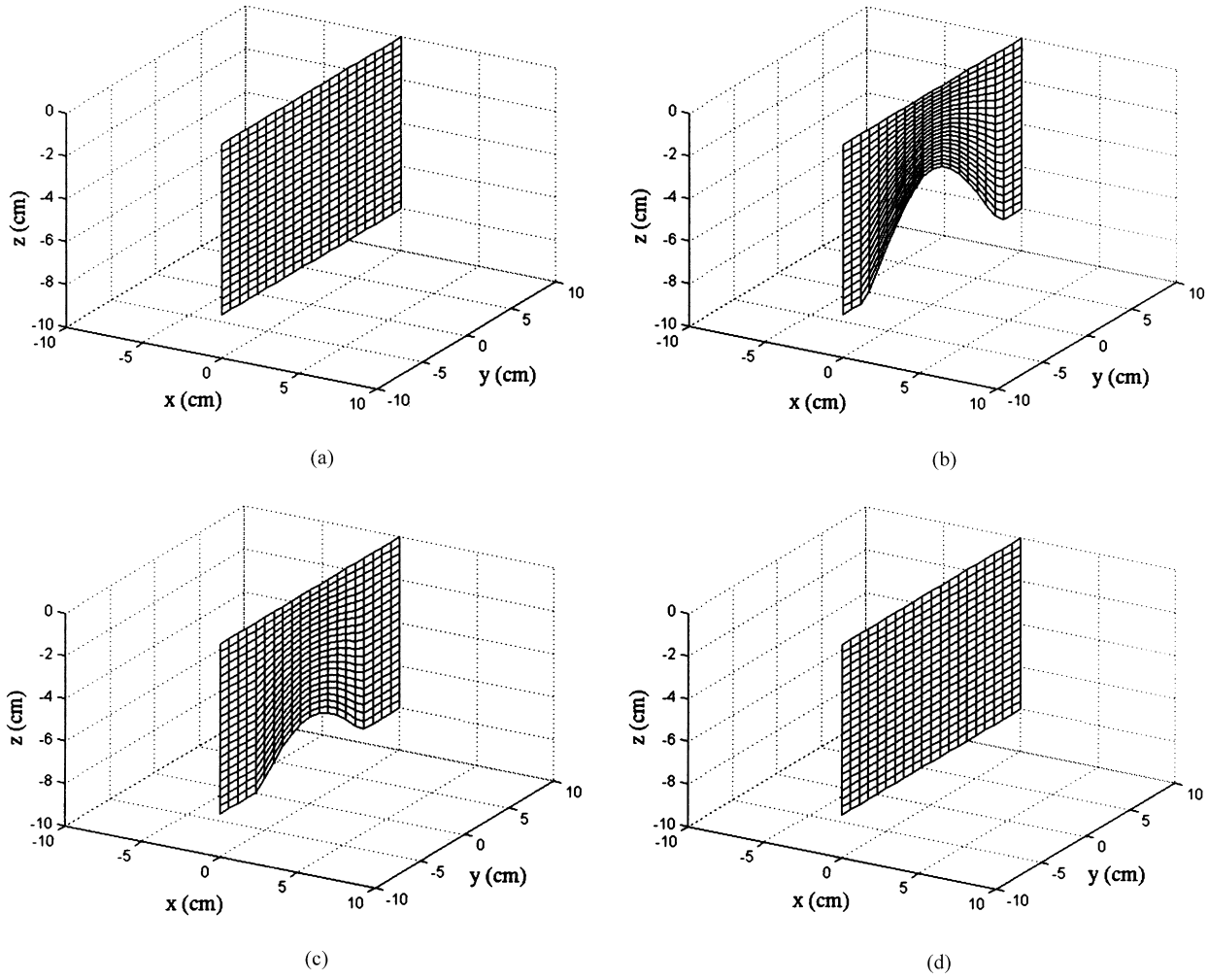

Fig. 6. Scan image of the vertical crack with constant depth: (a) no rebar, (b) $H = 4$ cm, (c) $H = 6$ cm, (d) $H = 8$ cm.

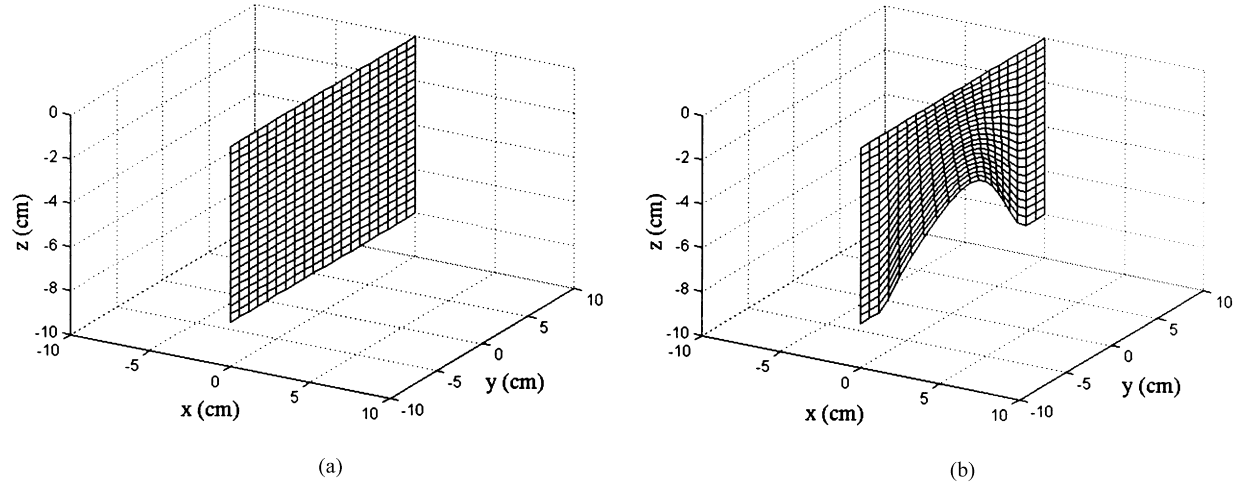

Fig. 7. Scan image of the vertical crack, asymmetric test layouts: (a) no rebar, (b) $H = 4$ cm.

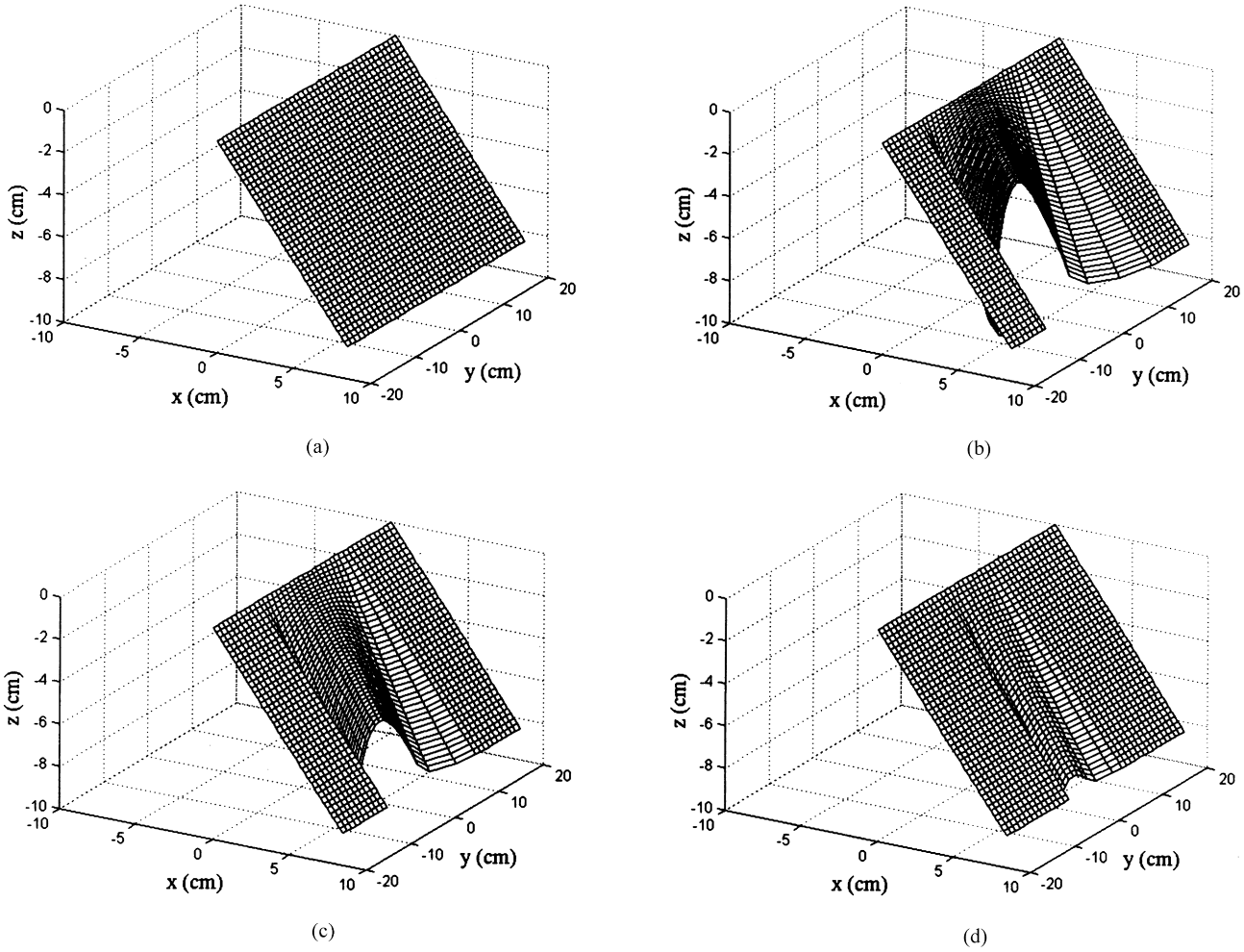

Fig. 8. Scan image of the 45° crack with constant depth: (a) no rebar, (b) $H = 4$ cm, (c) $H = 6$ cm, (d) $H = 8$ cm.

The occurrence of the warping phenomenon is useful. It can be used to determine whether the concavity of the image is due to the presence of the rebar or the actual shape of the crack edge. If the actual crack edge is concave and no rebars exist, there should be no warping even when asymmetric test layouts are adopted. On the other hand, if there is a rebar, different warping phenomena will be observed when different test layouts are used. Hence, one can use both the concavity of the crack edge and warping of the crack image to judge if the crack has propagated through a rebar.

4.2. Inclined crack with constant depth

Consider a reinforced concrete block with a 45° surface-opening crack. Such cracks are very common in concrete structures. Assume a crack length of 12 cm. The results of the scan are shown in Fig. 8.

Similar phenomena as seen above can be observed in this case. A correct image of the crack is constructed when there is no rebar, and the image is distorted when the rebar is present. It becomes concave above the rebar and recovers straight when the test section is away from the rebar. In addition, the distortion of the image is reduced as the covering thickness increases. However, the crack image does not remain plane when the rebar exists. This is because the test layouts are asymmetric with respect to the crack edge.

Fig. 9 shows the variation of the dip angle and the depth of the crack image as $H = 4$ cm. It is seen that the dip angle of the crack image is not a constant 45°. Instead, the curve is more like the letter "W" with the center of the W pinpointing the rebar coordinates. The rebar can also be located by examining Fig. 9(b). The depth of the crack image at $y = 0$ cm is 3.5 cm, which is shortest along the crack. This indicates that the rebar is located at $y = 0$ cm with a covering somewhat thicker than 3.5 cm.

4.3. Inclined crack with varying depth

Consider an inclined crack with varying depth in the reinforced concrete block. The geometry of the crack is as shown in Fig. 5, where $u_1 = 8$ cm, $v_1 = -20$ cm, $w_1 = 8$ cm, and $v_2 = 30$ cm. The covering thickness of the rebar is $H = 4$ cm. The results of the scan are as shown in Fig. 10.

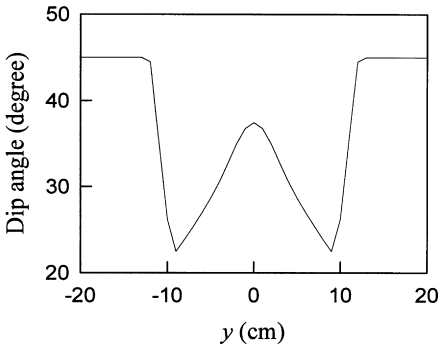

(a)

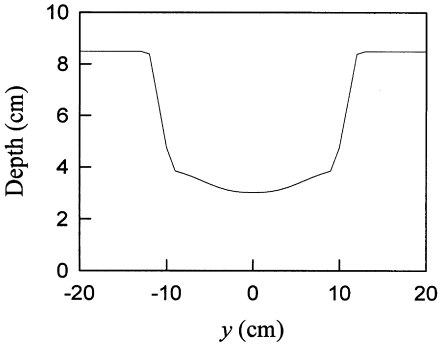

(b)

Fig. 9. (a) Dip angle and (b) depth of the crack image, $H = 4$ cm.

Again, concavity of the crack edge and warping of the crack image are observed around the rebar in this case.

5. Model test

The ability of the proposed method to scan a real crack was examined by a model test. The experiments were conducted on a concrete specimen with an embedded rebar as shown in Fig. 11. The specimen had a vertical slit with a constant depth of 12 cm. The covering thickness and diameter of the rebar were 4 and 2 cm, respectively. The longitudinal wave velocities of concrete and rebars were 4160 and 5863 m/s, respectively.

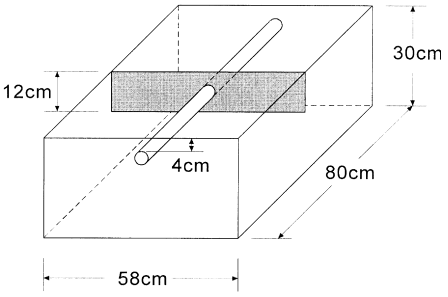

Fig. 11. Reinforced concrete model.

A vertical point source was generated by dropping a small steel ball (4.75 mm in diameter) on the surface of the specimen. An NBS conical transducer was used to measure the vertical displacement on the surface of the specimen. The sampling rate was 10 MHz.

In the experiment, the source and receiver were located at $x = -2$ and 8 cm, respectively, in the first test and at $x = 2$

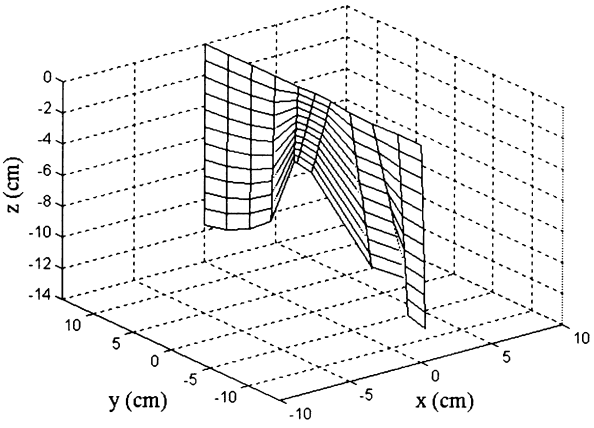

Fig. 12. Scan image of the model crack.

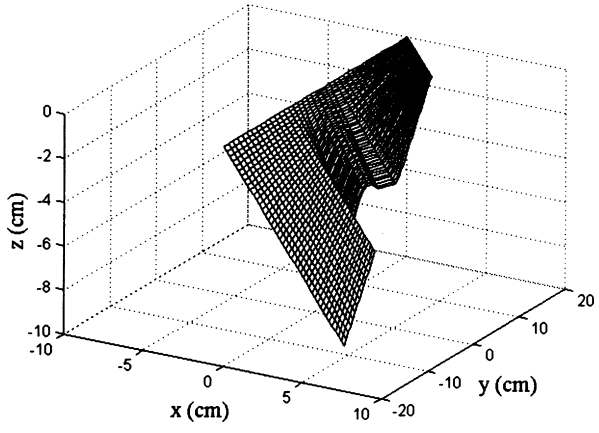

Fig. 10. Scan image of the inclined crack with varying depth.

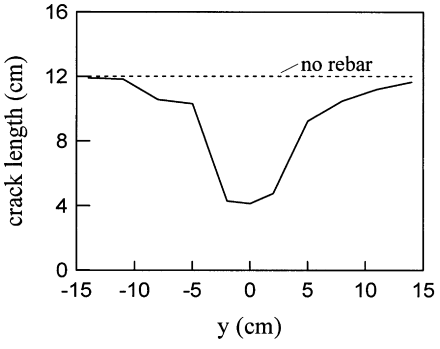

Fig. 13. Depth of the crack image.

and −8 cm, respectively, in the second test. The coordinate system was the same as shown in Fig. 5. The test sections were perpendicular to the crack opening and the distance between successive test sections was 2 cm.

The scan image of the crack around the rebar is shown in Fig. 12. As expected, the crack edge is concave around the rebar. The depth of the crack image is shown in Fig. 13. It is seen that the crack length is approximately equal to the covering thickness 4 cm right above the rebar. The crack length increases as the test section is moved away from the rebar. Finally, the image restores its correct length when the deviation of the test section is about 13 cm. This is consistent with the value 12.19 cm as predicted using Eq. (9).

Similar to the numerical examples, the location and the covering thickness of the rebar can be determined by the depth curve of the crack edge.

6. Conclusions

This paper develops a method to scan the surface opening cracks of reinforced concrete. Three numerical examples and a model test are presented to illustrate the effectiveness of the proposed method. Several conclusions can be drawn from this study:

1. When the travel time of the first arrival signal is not affected by the rebar, a correct crack image can be constructed.
2. Concavity of the crack edge and warping of the crack plane indicate a high probability that the crack has propagated through a rebar.
3. The apex of the concavity of the crack edge can be used to determine the location of the rebar.
4. The depth of the crack image at the apex of the edge concavity gives a conservative estimate of the covering thickness of the rebar.

Acknowledgements

This work was supported by the National Science Council, Taiwan, Republic of China under Grant NSC NSC 88-2625-Z-002 F-012.

References

[1] Sakata Y, Ohtsu M. Crack evaluation in concrete members based on ultrasonic spectroscopy. ACI Materials Journal 1995;92(6): 686–98.
[2] Chang YF, Wang CY. A 3-D image detection method of a surface opening crack in concrete using ultrasonic transducer arrays. Journal of Nondestructive Evaluation 1997;16(4):193–203.
[3] Wu TT, Fang JS, Liu PL. Detection of the depth of a surface-breaking crack using transient elastic waves. Journal of the Acoustic Society of America 1995;97(3):1678–86.
[4] Lin Y, Su WC. The use of stress waves for determining the depth of surface-opening cracks in concrete structures. ACI Materials Journal 1996;93(5):494–505.
[5] Lin Y, Liou T, Hsiao C. Influences of reinforcing bars on crack depth measurement by stress waves. ACI Materials Journal 1998;95(4):407–18.
[6] Liu PL, Tsai CD, Wu TT. Imaging of surface-breaking concrete cracks using transient elastic waves. NDT&E International 1996;29(5):323–31.
[7] Kuo MK, Lin TR, Liu PL, Wu T-T. Locating the crack-tip of a surface-breaking crack. Part I. Line crack. Ultrasonics 1998;36: 803–11.
[8] Lee K-H. A study on the detection of surface-opening cracks in reinforced concrete. Master's dissertation. Institute of Applied Mechanics, National Taiwan University, 1998.